Korean J. Chem. Eng., 39(2), 316-327 (2022)
DOI: 10.1007/s11814-021-0932-z

pISSN: 0256-1115
eISSN: 1975-7220

Effect of non-uniform magnetic field on mixing index of a sinusoidal micromixer

Dariush Bahrami, Afshin Ahmadi Nadooshan†, and Morteza Bayareh

Engineering Faculty, Shahrekord University, Shahrekord, Iran
(*Received 30 March 2021 • Revised 24 July 2021 • Accepted 17 August 2021*)

Abstract−Magnetic fluid micromixers are widely used in medical diagnostic processes, food processing, and biochemical engineering. In the present study, a two-dimensional combined active/passive micromixer was designed and evaluated to perform experimental investigation for $0.1<Re<0.7$. The microchannel walls are sinusoidal and a neodymium magnet is placed close to the microchannel. The results demonstrate that the magnetic field improves the mixing quality by 17.5%. It is concluded that the performance of the micromixer with sinusoidal walls is 1.16 times higher than one with a straight channel. The results show that as the volume fraction of magnetic nanoparticles is enhanced, the mixing index is intensified. For instance, the degree of mixing is increased by 24% when the volume fraction enhances from 0.015% to 0.06%. Besides, as the magnet is placed closer to the microchannel, the mixing index is enhanced. The maximum mixing index occurs when the magnet is 13.75 mm from the inlets.

Keywords: Microfluidics, Micromixer, Magnetic Force, Ferrofluid, Sinusoidal Wall

INTRODUCTION

Microfluidic devices have widespread applications in industrial and scientific contexts, such as drug delivery and chemical and biological syntheses [1]. Micromixing is one of the applications of these devices that can be classified into active and passive systems. In active methods, external forces, including acoustic field [2], electric field [3], electrokinetic [4], electromagnetic field [5], and magnetic field [6] are needed to improve mixing quality. When a magnetic field is applied to a microchannel, two issues are of particular importance. First, the fluid entering the microchannel must be a ferrofluid. Second, a uniform or non-uniform magnetic field is required to affect a ferrofluid. Active methods require specific and expensive equipment; however, the application of the magnetic field does not require specific tools. The use of a permanent magnet is more economical than other active methods. In addition, the magnetic force has special applications in medical and biomedical areas, such as drug delivery, and cancer cell isolation [7].

Numerous studies have been conducted in the field of magnetic micromixers. In these investigations, the impact of uniform and non-uniform magnetic field, magnetic field strength, the volume fraction of ferrofluid, size of nanoparticles, etc. on the mixing process was evaluated. Hejazian et al. [8] designed a micromixer with three inlets and an output. They applied a non-uniform magnetic field by placing three magnets one millimeter from the main channel. Their numerical and experimental results showed that there is the highest concentration gradient in the center of the micromixer without applying a magnetic field. In this case, the concentration is only a function of the velocity and viscosity of the fluid. Hejazian and Nguyen [9] investigated the impact of a non-uniform magnetic field, volume fraction of nanofluid, and inlet flow rate on mixing performance and reached a mixing efficiency of 88%. They found that the mixing index is enhanced by increasing the nanofluid volume fraction and decreasing the inlet flow rate. Wang et al. [10] studied mixing quality in a microchannel in which the ferrofluid flow enters from its central entrance and the silicon-oil flow enters as a sheath flow numerically and experimentally. They used a uniform magnetic field with strengths of 0, 8, 12, 16, and 30 mT to increase the mixing index, and showed that when the magnetic field reaches its critical value, the ferrofluid flow spreads to the oil silicon. It was shown that a further increase in the magnetic field leads to an unstable structure. Wen et al. [11] reached rapid macromixing using an electromagnetic field and achieved a mixing index of 95% in 2 s. Their microchannel was 3.5 cm long and a magnet was located 1 mm from the microchannel. He et al. [12] investigated the effect of magnetic field on unlabeled nonmagnetic particles and demonstrated that ferrofluid concentration, the strength of the magnetic field and its distribution, inlet mass flow rate, and particle size affect the flow deflection in a microchannel. Munir et al. [13] investigated the effect of nanoparticle diameter and inlet velocity on mixing quality and reported that when the diameter of nanoparticles reaches from 100 to 300 nm, their diameter does not have a significant effect on the mixing index and found that maximum mixing efficiency occurs for 300 μm/s. Saadat et al. [14] studied the effect of the magnetic force on the microchannel and found that as the frequency increases, the mixing index is reduced. They also reported the maximum mixing index of 97% at 1.5 s. Azimi et al. [15] investigated the effect of Fe_3O_4 magnetic nanoparticles on mass transfer of a two-phase flow in the presence of a magnetic field with a magnitude of 0.15 T in a Y-shaped micromixer. They revealed that the closer the magnet is to the channel, the more mass transfer of the liquids. Nouri et al. [16] numerically and experimentally investigated the mixing process in a Y-shaped microchannel using a permanent magnet. They found that when the strength of the magnetic field changes from 0.125 to 0.22 T, it has a significant effect on the mixing of fluid and ferrofluid, while this effect is not signif-

†To whom correspondence should be addressed.
E-mail: ahmadi@sku.ac.ir

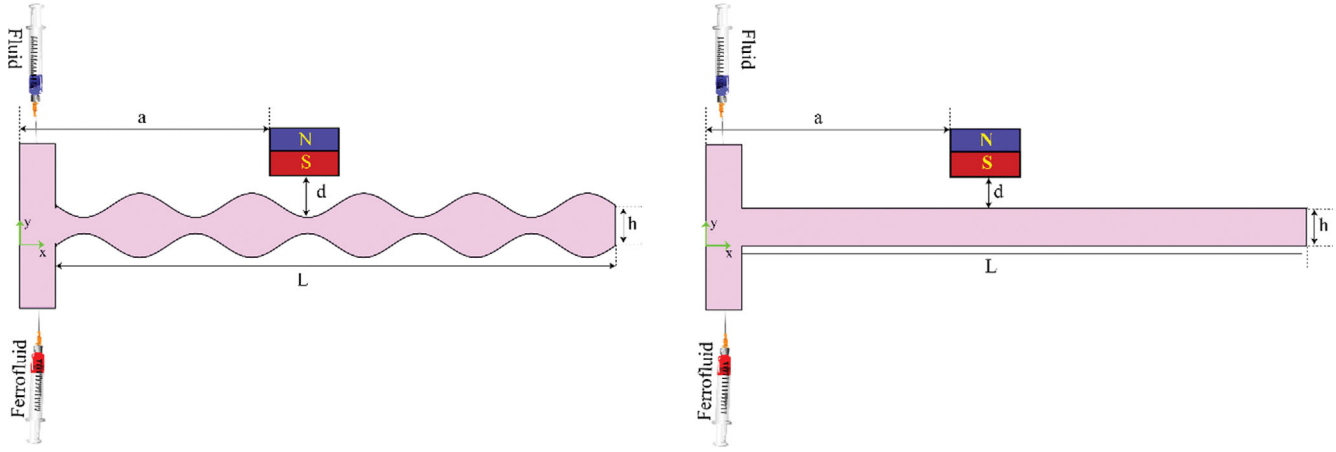

Fig. 1. Schematic of the problem.

icant by increasing the strength of the magnetic field from 0.22 to 0.3 Zhou and Nguyen [17] demonstrated that the numerical and simulation results exhibit the same behavior for the mixing of ferrofluid and oil under uniform magnetic field. It was shown that magnetofluidic phenomenon is caused by the increase of the apparent diffusion due to the drift of the magnetic particles and secondary flow in the interface between ferrofluid and the oil.

In passive methods, mixing takes place without external forces using complex structures [1,18]. Since there are numerous geometries for passive micromixers, some previous researchers who considered curved microchannels are reviewed. Parsa et al. [19] studied a sinusoidal micromixer numerically and experimentally and showed that symmetrical vortices are formed in the convergent throat area, which is the result of centrifugal force and significantly affects the mixing index. Hossain et al. [20] numerically simulated three zigzag, square-wave, and curved micromixers and revealed that at small Reynolds numbers (Re<<1) mixing is due to molecular diffusion. Javaid et al. [21] designed microchannels by combining sinusoidal walls and spiral microchannels. They found that the mixing index increased when the Reynolds number exceeded 30 due to the generation of secondary flow. Usefian and Bayareh [22] proposed a micromixer with convergent-divergent walls and reached a mixing efficiency of about 100%. They concluded that the formation of vortices is the main factor to improve the mixing performance. Afzal and Kim [23] designed a divergent-convergent microchannel using sinusoidal walls and showed that the mixing index of the convergent microchannel is 67% higher than that of the straight channel. Mondal et al. [24] investigated the effect of the sinusoidal wall on the mixing of two liquids and found that the mixing index in the raccoon model is higher than that in the serpentine one.

Almost all numerical and experimental investigations have employed conventional nanoparticles to enhance the mixing quality in the presence of magnetic force. Magnetophoretic micromixers can use novel materials, nanoparticles, and various bi-composites [25-28].

According to a literature review, it can be concluded that active micromixers use simple geometries, while passive ones employ complex geometries. The geometry of the proposed hybrid micromixer with sinusoidal walls is relatively simple due to the ease of fabrication. In other words, this micromixer has a relatively simple geometry and high mixing efficiency. In the present study, a two-dimensional combined active/passive micromixer was proposed to mix fluid and ferrofluid. The T-shaped micromixer has sinusoidal microchannel walls and a permanent magnet is placed in the vicinity of the channel. The effect of inlet flow, ferrofluid volume fraction, and magnet distance from the channel on the mixing process was investigated.

PROBLEM DESCRIPTION

In the present study, T-shaped microchannels with straight and sinusoidal walls were compared when the micromixers are affected by a nonuniform magnetic field (Fig. 1). The height of the present mixer is equal to 500 μm and its length is 35 mm. To generate a magnetic field, a neodymium magnet with dimensions of 5×5×5 mm^3 and magnetism of 9.55×10^5 A/m [29] was placed at different distances from the microchannel. Fluid and ferrofluid flow enters the microchannel with flow rates of 12.5, 25, 50, and 75 μl/min (0.1<Re<0.7, where $\mathrm{Re}=\frac{\rho_f U_m D_h}{\mu_f}$) and volume fractions of 0.015, 0.03, and 0.06%.

GOVERNING EQUATIONS

To simulate the mass transfer process in the presence of a magnetic field, continuity and Navier-Stokes equations for the flow field, Maxwell equations for the magnetic field, and the mass transfer equation for the species should be solved.

Continuity and Navier-Stokes equations for steady and incompressible flow are as follows:

$$\nabla\cdot\vec{u}_f=0 \tag{1}$$

$$\nabla[-\mathrm{PI}+\mu_f(\nabla\vec{u}_f+(\nabla\vec{u}_f)^T)]-\rho_f(u_f\cdot\nabla)u_f+\vec{F}_{ext}=0 \tag{2}$$

where

$$\vec{F}_{ext}=\vec{F}_g+\vec{F}_{st}+\vec{F}_m \tag{3}$$

$$\vec{F}_m = \mu_0 (M \cdot \nabla)\vec{H} \tag{4}$$

where $\vec{u}_f$ is velocity vector, ρ_f and μ_f are fluid density and dynamic viscosity, respectively. $\vec{F}_{ext}$ is the external force and is added to the Navier-Stokes equation as a source term. $\vec{F}_{ext}$ involves the gravitational force $\vec{F}_g$, surface tension $\vec{F}_{st}$, and magnetic force $\vec{F}_m$. It can be assumed that $\vec{F}_g$ and $\vec{F}_{st}$ are zero [16,18].

The density and viscosity of nanofluid are calculated as follows [30,31]:

$$\rho_{ff} = (1-\varphi)\rho_w + \varphi\rho_{np} \tag{5}$$

$$\mu_{ff} = \mu_w \left(\frac{1}{(1-\varphi)^{0.25}} \right) \tag{6}$$

where ρ_{ff} and μ_{ff} are fluid density and dynamic viscosity, respectively. Note that when the fluid and ferrofluid enter the microchannel, their viscosity, and density change during the mixing process as follows:

$$\rho_{mix} = (1-C)\rho_{w+} C\rho_{ff} \tag{7}$$

$$\mu_{mix} = \mu_{ff} e^{R(1-C)} \tag{8}$$

$$R = \mathrm{Ln}\left(\frac{\mu_w}{\mu_{ff}} \right) \tag{9}$$

To solve the volumetric magnetic force the Maxwell equations should be solved [32]:

$$\nabla \cdot \vec{B} = 0 \tag{10}$$

$$\nabla \times \vec{H} = 0 \tag{11}$$

$$\vec{B} = \mu_0 (\vec{H} + \vec{M}) \tag{12}$$

$$\vec{B} = \nabla \times \vec{A} \tag{13}$$

$$\vec{M} = \vec{M}_0 C = \chi \vec{H} C \tag{14}$$

where $\vec{B}$ is the flux passing through the surface, μ_0 is the vacuum permeability coefficient and has a constant value. $\vec{H}$, $\vec{M}$, and $\vec{A}$ are the magnetic field strength, the ferrofluid magnetism, and the electric potential vector, respectively. When a magnetic particle is exposed to a magnetic field, its magnetization before saturation is calculated using Eq. (14), in which $\vec{M}_0$ and χ are the initial magnetization and magnetizability, respectively.

The advection-diffusion equation should be solved for the mass transfer of species [8]:

$$\vec{u}_{np} \cdot \nabla c_{np} + \nabla \cdot (-D \nabla c_{np}) = R_{np} \tag{15}$$

where R_{np} is the production rate of the species and because there is no reaction in the present simulations, R_{np}=0. D is the diffusion coefficient and $\vec{u}_{np}$ is the particle velocity:

$$\vec{u}_p = \vec{u} + \vec{u}_{mag,\,np} \tag{16}$$

$$\vec{u}_{mag,\,np} = \frac{\vec{F}_{mag,\,np}}{6\pi\eta r_{np}} \tag{17}$$

where

$$\vec{F}_{mag,\,np} = (\vec{m} \cdot \nabla)\vec{B} \tag{18}$$

$$\vec{m} = V_p \vec{M} \tag{19}$$

$$\vec{M} = \Delta\chi \vec{H} \tag{20}$$

$$\vec{F}_{mag,\,np} = \frac{V_p (\Delta\chi)(\vec{B} \cdot \nabla)\vec{B}}{\mu_0} \tag{21}$$

where $\vec{F}_{mag,\,np}$ is the magnetic force and $\vec{m}$ is the total momentum exerted on the particle, which depends on the volume of the particle V_p and its magnetism $\vec{M}$. $\Delta\chi$ is the difference in the magnetization of the fluid and the nanoparticles. In magnetic micromixers, $\vec{u}_p$ can be considered equal to u because the size of $\vec{u}_p$ is very small compared to u [33].

Eq. (22) is used as a criterion for mixing [34]:

$$\eta = \left(1 - \frac{\int_0^h |c - c_\infty| dy}{\int_0^h |c_0 - c_\infty| dy} \right) \times 100 \tag{22}$$

Two species, A and B, enter the micromixer with different concentrations. η is the mixing index and $c_\infty = (c_A + c_B)/2$. Also, c_0 is the initial concentration, which is zero for water and one for ferrofluid. Table 2 presents the value of constant parameters.

Table 1. Pressure drop for straight and sinusoidal micromixers

Mass flow rate, μl/min	Pressure drop, Pa	
12.5	0.844	2.546
25	1.688	5.093
50	3.762	10.186
75	5.065	15.281

Table 2. Parameters and their values used in the present simulations

Density of water, kg/m^3	ρ_f	998.2
Viscosity of water, Pa·s	μ_w	0.00089
Diameter of nanoparticles, nm	d_{np}	30
Density of nanoparticles, kg/m^3	ρ_{np}	5.18
Temperature, °C	T	25
Diffusivity coefficient (m^2/s)	D	3.14×10^{-10}
Susceptibility	χ	0.5
Permeability of the vacuum, N/A^2	μ_0	$4\pi\times10^{-7}$

NUMERICAL IMPLEMENTATION AND GRID STUDY

Governing equations are solved using the finite element method (FEM) by employing COMSOL Multiphysics. P2+P1 discretization scheme is used for Navier-Stokes equations and second-order quadratic equations are employed for mass transfer equations. A fully developed laminar flow is imposed on the inlet of the channel and outlet pressure (p_g=0) boundary condition is employed for the outlet of the channel. Besides, a no-slip boundary condition is considered for channel walls.

Since the fluid flow, Maxwell, and mass transfer equations are

Table 3. Mixing efficiency calculated for different grid resolutions

Number of elements	ME (%)	Error (%)
79,503	83.02	-
92,179	78.88	4.9
124,224	73.35	7
194,022	**73.10**	**0.34**
278,411	73.103	0.004
328,261	73.103	0

solved, the selection of the grid is very important. A structured grid is used inside the microchannel, which contains fluid and nanofluid. The finer grid resolution is used in the vicinity of the walls. Table 3 presents the results related to fluid and nanofluid flows with a flow rate of 25 μl/min and a volume fraction of 0.03% in the presence of a magnetic field for different grid resolutions. It can be seen that when the number of elements increases from 194022 to 278411, there is no significant difference in the value of the mixing index, showing that the grid resolution of 194022 is sufficient for the simulations.

VALIDATION

To validate the results of the present numerical solutions, the present results were compared with the experimental data of Nouri et al. [16] who investigated the mixing process in a Y-shaped microchannel saturated with magnetic ferrofluid. Fig. 2 compares the results obtained from the numerical results and experimental data of Nouri et al. [16] for a volume fraction of 0.03% and an inlet flow rate of 60 ml/min when a permanent magnet with a strength of 0.3 T is placed at a distance of 1 mm from the micromixer. In addition, to perform further validation, the results of He et al. [12] were also verified and shown in Fig. 3. This figure shows the magnetic field strength in the center of a microchannel along its length created by a uniform magnetic field. As it is observed, the numerical results are in good agreement with those of Nouri et al. [16] and

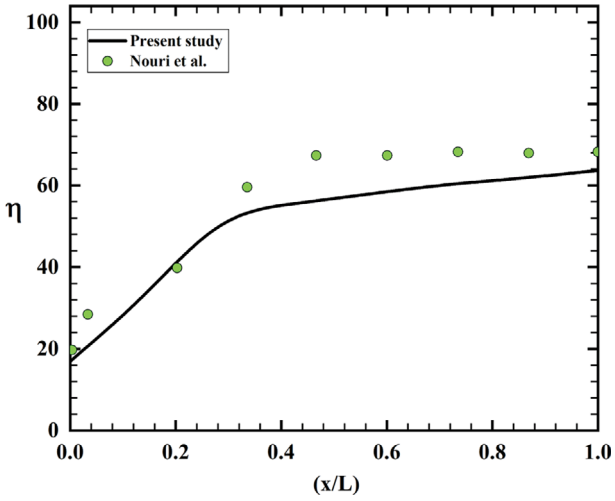

Fig. 2. Mixing efficiency along the microchannel.

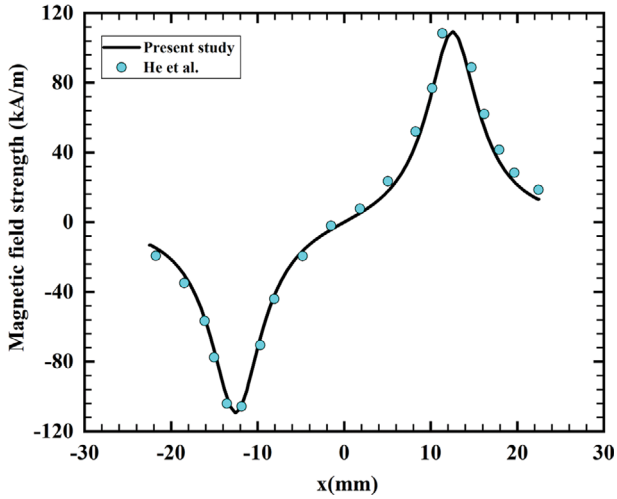

Fig. 3. Magnetic field strength along the channel length.

He et al. [12].

RESULTS

A magnetic field has many microscale applications, including pumping flow [35-37], mixing [38], and particle separation [39]. This study evaluated the effect of a magnetic field created by a permanent magnet on the mixing of water and ferrofluid to fabricate a PDMS microchip. For this purpose, the effect of a non-uniform magnetic field on the mixing quality in a micromixer with sinusoidal walls was investigated and compared with the one with straight microchannels. Besides, the effect of nanofluid volume fraction, inlet flow rate, and magnet distance from the microchannel on the mixing index was investigated. The pressure drop is an important factor in micromixer designs. Table 1 shows the values of the overall pressure drop that is the difference between the area-averaged total pressure at the inlet and outlet of the mixing channel. As expected, the sinusoidal mixer has a higher pressure drop than the one with a straight channel.

1. Effect of the Magnetic Field

To determine the effect of the magnet on the mixing of the two fluids, the streamlines are shown in Fig. 4 with and without a magnet. According to this figure, in the absence of a magnetic field, the

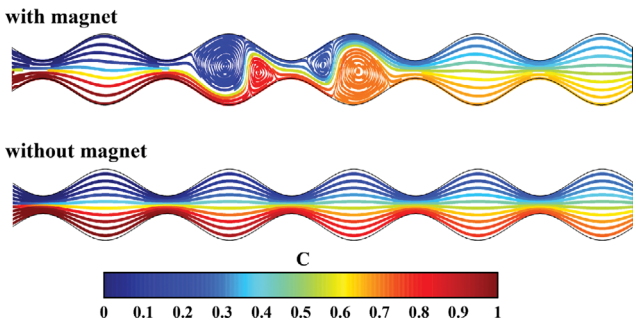

Fig. 4. Effect of magnetic field on streamlines along the microchannel at φ=0.03%, d=1,000 μm, a=13.75 mm, and $\dot{Q}$=25 μl/min.

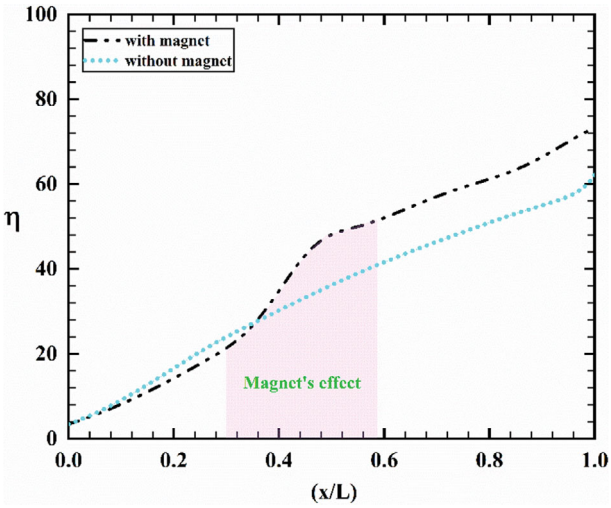

Fig. 5. Mixing index along the microchannel with and without the magnetic field at φ=0.03% and $\dot{Q}$=25 μl/min.

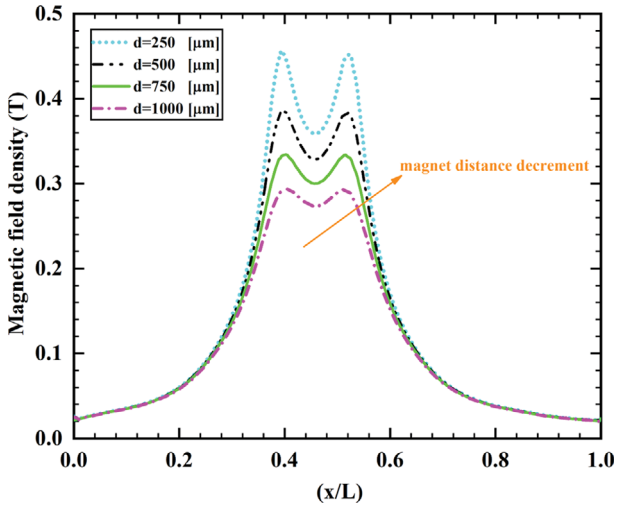

Fig. 6. Magnetic field density in the centerline of the microchannel for different distances from the microchannel.

streamlines are parallel and the mixing rate is very low due to the molecular diffusion. However, as a magnet is placed close to the channel, some vortices are formed where the magnetic field is applied. Since the ferrofluid has magnetic property, the magnet attracts the ferrofluid. The attraction of ferrofluid causes the other fluid to be directed downwards and eventually leads to the formation of a vortex. It is clear that mixing quality is increased in this area.

Fig. 5 shows the mixing index at a flow rate of 25 μl/min and a volume fraction of 0.03%. It is demonstrated that when there is no magnet, the mixing index gradually increases due to molecular diffusion. However, when the magnetic field is generated (highlighted area), the mixing index increases sharply. This is due to the disturbances created by the magnetic field. In fact, the resulting disturbances cause the formation of vortices, leading to an enhancement in the mixing of two fluids. The results show that the mixing index at the outlet of the magnetic micromixer is 17.5% higher than that for the micromixer when the magnetic field in not applied.

2. Effect of Vertical Distance of Magnet from Microchannel (d)

In this section, the effect of the distance of the permanent magnet from the microchannel was investigated. Fig. 6 shows the magnetic field strength of the magnet when it is located at various distances of 0.25, 0.5, 0.75, and 1 mm from the microchannel. It can be seen that as the distance between the magnet and the microchannel increases, the strength of the magnetic field within the microchannel decreases. There are two maximum points for each case, indicating two magnetic corners. Fig. 7 shows the distribution of the magnetic field within the PDMS and microchannel environments. It is revealed that the maximum strength of the magnetic field occurs in the area near the magnet and decreases with the distance from the channel. Streamlines indicate the direction of the magnetic field in such a way that the field enters the negative pole and exits from the positive one.

Fig. 8 shows the effect of magnet distance from the channel on the mixing index for φ=0.03% and different flow rates. According to this figure, as the distance between the magnet and channel increases, the mixing index along the microchannel is reduced. This is because the strength of the magnetic field is reduced with the distance between the magnet and channel, leading to a reduction

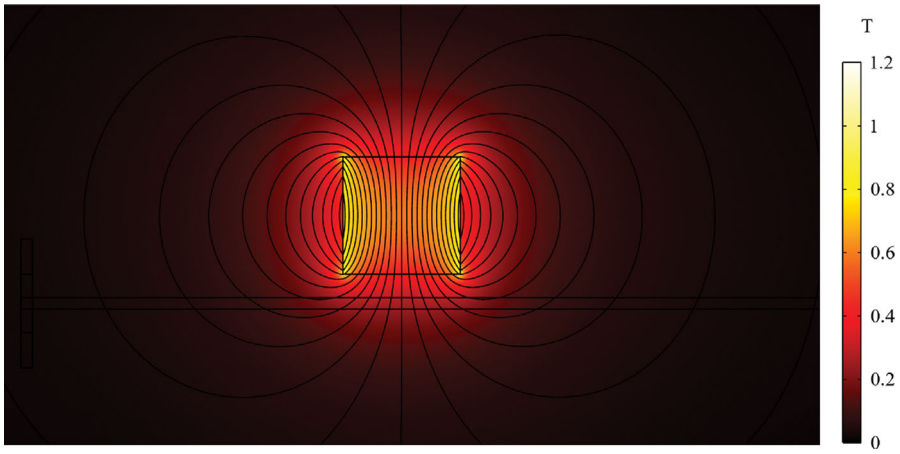

Fig. 7. Distribution of magnetic field density for a distance of 1 mm from the microchannel.

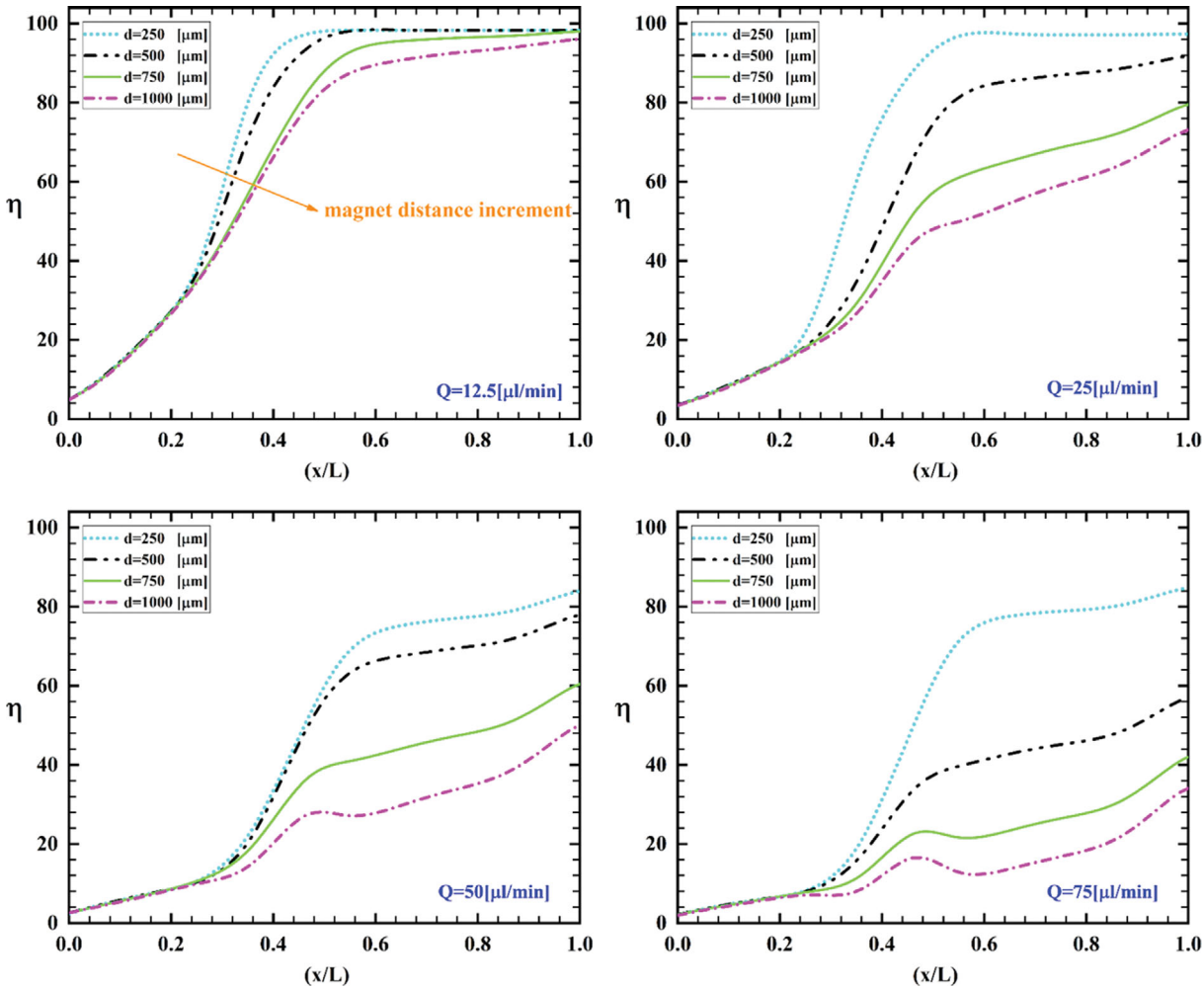

Fig. 8. Mixing index along the microchannel for different distances of the magnet from the channel at φ=0.03% and a=13.75 mm.

in the magnetic force on the ferrofluid. Fig. 9 illustrates how the distance of the magnet from the channel affects the strength of the magnetic force, the flow pattern, and the mixing of fluids. The size of the vortices is enhanced as the magnet approaches the microchannel due to the greater magnetic force. At low flow rates, the vortex occupies the entire height of the microchannel.

Fig. 10 shows that when the magnet distance from the channel increases from 250 to 1,000 μm, the mixing index decreases by 2%, 33%, 67%, and 148% for flow rates of 12.5, 25, 50, and 75 μl/min, respectively. Besides, it can be observed that when the magnet is located at a distance of 250 μm from the microchannel, the difference between the values of mixing at the outlet is about 1% for the flow rates of 12.5 and 25 ml/min and also for the flow rates of 25 and 50 ml/min.

3. Effect of Horizontal Distance of Magnet from the Inlets (a)

Since the microchannel wall is convergent-divergent, the impact of the magnetic field should be checked if the magnet is placed at the top of the convergent part (for instance, a=13.75 mm) or the top of the divergent part (for example, a=17.25 mm) or the distance between the convergent and the divergent parts (for instance, a=16.25 mm). Fig. 11 shows the effect of the horizontal distance for flow rates of 12.5, 25, 50, and 75 μl/min when φ=0.03% and d=1,000 μm. for the case in which the magnet is placed at a distance of a=13.75 mm, four vortices are formed in the two convergent regions after and before the magnet location. Vortices formed at distances of 16.25 mm and 17.25 mm act almost the same. In the convergent and divergent region, which is close to the magnet for a=17.25 mm, two vortices with approximately the same size are formed, and in the convergent and divergent region after and before the magnet, two vortices are formed in the ferrofluid and water separately. As the flow rate increases, the vortices are weakened and disappear. Thus at a very high flow rate, the number of vortices reduces from four to two small vortices. In the convergent and divergent region, which is close to the magnet, two different-size vortices are formed when a=16.25 mm. Hence, increasing the flow rate causes two vortices to form in the fluid. The maximum mixing index occurs when the magnet is at a distance of a=13.75 mm from the inlets (Fig. 12).

4. Effect of Sinusoidal Wall

In this section, the mixing quality of the micromixer with sinusoidal walls was compared with that of the mixer with straight walls under the same conditions: Q=25 μl/min and φ=0.03%. Accord-

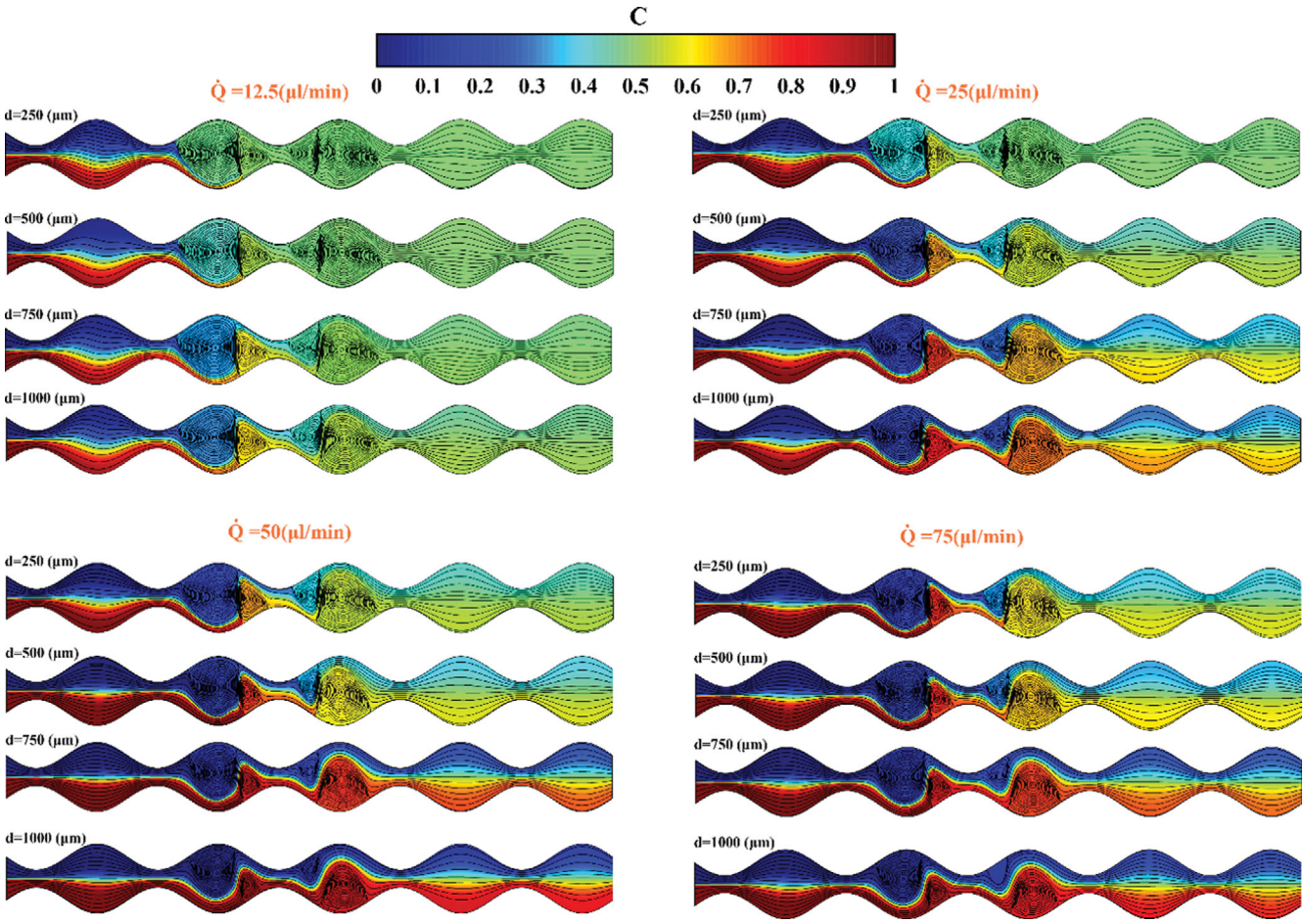

Fig. 9. Effect of magnet distance from the channel on mixing quality at φ=0.03% and a=13.75 mm.

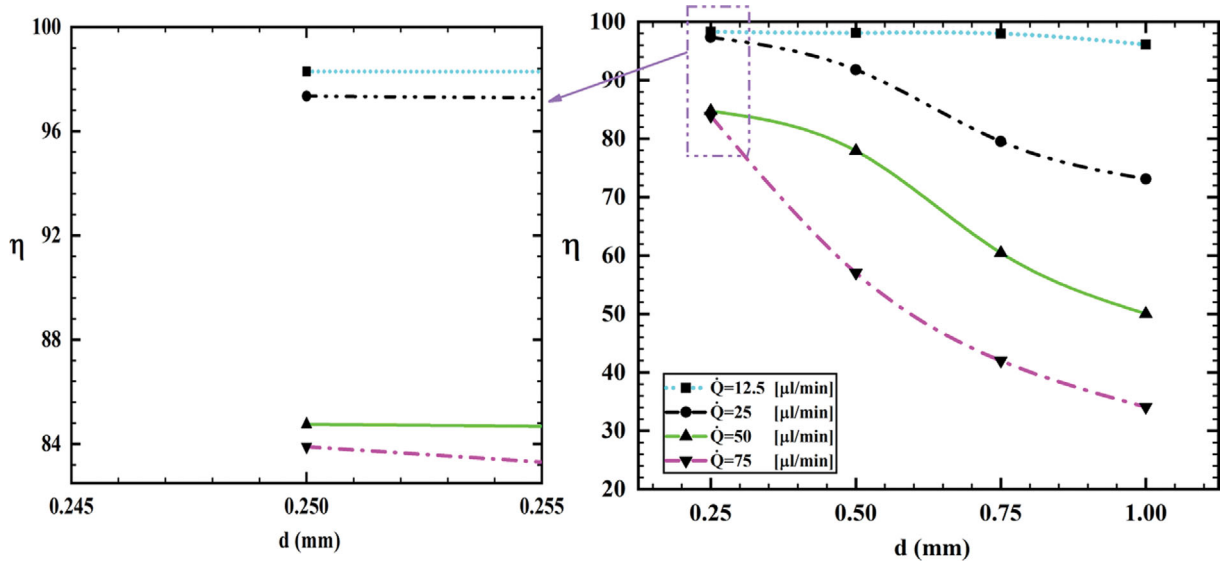

Fig. 10. Effect of magnet distance from the channel on the mixing index at φ=0.03% and a=13.75 mm.

ing to Fig. 13, the mixing index is 73% and 68% for the micromixer with sinusoidal walls and straight walls, respectively. When the wall of a microchannel is sinusoidal, the centrifugal force created by the flow rotation due to the magnetic field becomes stronger, resulting in higher mixing quality. By comparing the vortices formed in the two microchannels, it can be seen that the width of

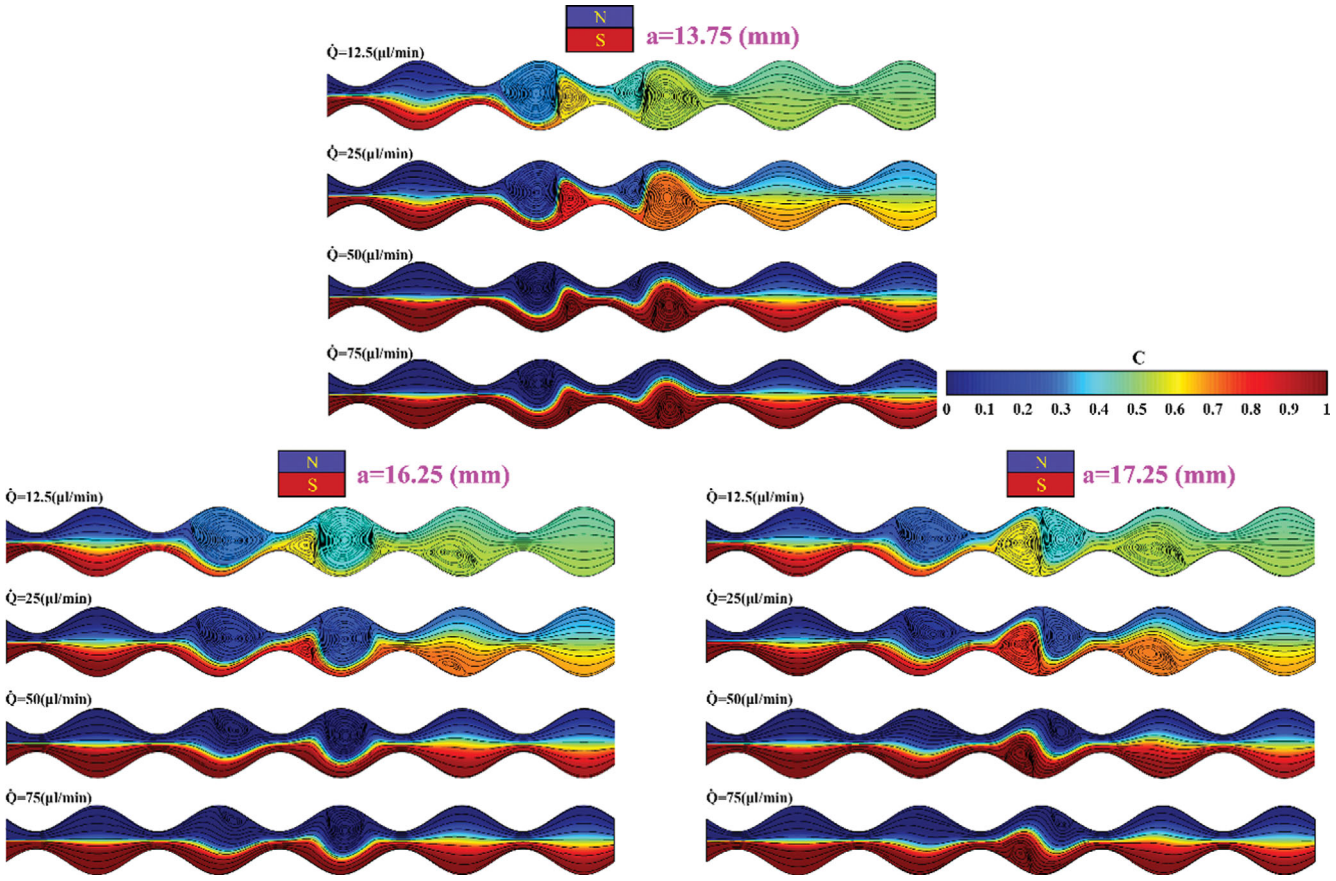

Fig. 11. Effect of the horizontal distance of the magnet from the inlets on concentration distribution and streamlines at φ=0.03% and d= 1,000 μm.

the vortices formed in the straight microchannel is greater.

Fig. 14 presents the ratio of the mixing index of the micromixer with sinusoidal walls to that of the micromixer with straight walls for different horizontal distances of the magnet from the inlet. For a flow rate of 12.5 μl/min, the molecular diffusion is the dominant mechanism of mixing and the effect of the sinusoidal wall is negligible. However, as the flow rate is enhanced, the mixing index increases, so that the mixing index is 4, 11, and 16% for the flow rates of 25, 50, 75 μl/min, respectively. It is noteworthy that when the flow rate changes from 25 to 50 μl/min, the mixing index increases by 7% higher; however, when it enhances from 50 to 75 μl/min, the mixing index is increased by 5%.

5. Effect of Nanoparticle Volume Fraction

The effect of nanofluid volume fraction is evaluated by considering three volume fractions of 0.015%, 0.03%, and 0.06% for the flow rate of 25 μl/min. Fig. 15 reveals that an increase in the volume fraction of nanoparticles improves the mixing index. Increasing the nanoparticle volume fraction leads to an increase in the magnetic force exerted by the magnetic field on the ferrofluid. The present observations are in agreement with the experimental results of Hejazian and Nguyen [8], who improved the mixing efficiency from 20% to 80% by increasing the nanofluid volume fraction. Fig. 16 shows that an increase in the volume fraction drastically reduces the mixing length. When the volume fraction changes from 0.015 to 0.03%, the mixing index is enhanced by 7%, and when the volume fraction varies from 0.03 to 0.06%, the mixing index increases by 15%.

6. Effect of Inlet Flow Rate

The effect of inlet flow rate on the mixing process of water and ferrofluid is shown in Fig. 17 for a volume fraction of 0.03%. By comparing the distribution of species and streamlines, it can be concluded that the most important factor affecting mixing is the formation of vortices caused by magnetic force. An enhancement of the inlet flow rate affects the formation of vortices. As the flow rate is enhanced, the vortex becomes weaker. It can be expressed that lower fluid velocity leads to stronger magnetic force, leading to the creation of stronger vortices. However, as the flow rate increases, the magnetic force is affected by the hydrodynamic force and its strength to form large vortices is weakened.

Fig. 18(a) shows the effect of the inlet flow rate on the mixing index for the volume fraction of 0.03%. At low inlet flow rates, the mixing index is high. This is because the mixing mechanism is molecular diffusion. Besides, the magnetic force strongly causes mass transfer from the ferrofluid flow to the water stream. Although mixing is high at low flow rates, the time required for the mixing is high. The mixing index decreases by increasing the inlet flow rate. The reason can be explained as follows: As the inlet flow rate increases, the momentum force is enhanced, leading to an increase in the hydrodynamic force. As a result, as the hydrodynamic force increases, the magnetic force cannot move the ferrofluid in the

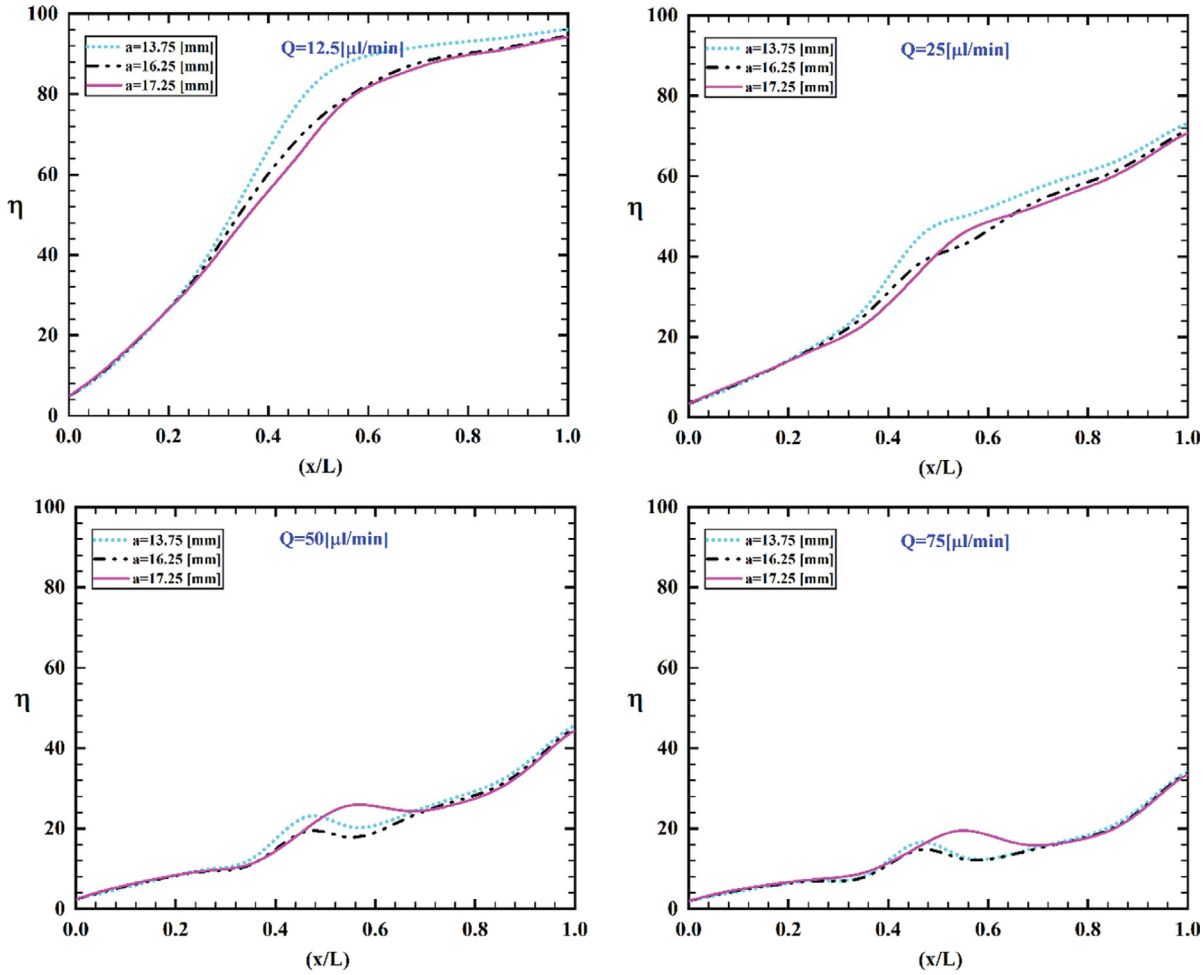

Fig. 12. Mixing index along the micromixer for different values of horizontal distance of magnet from the inlet at φ=0.03% and d=1,000 μm.

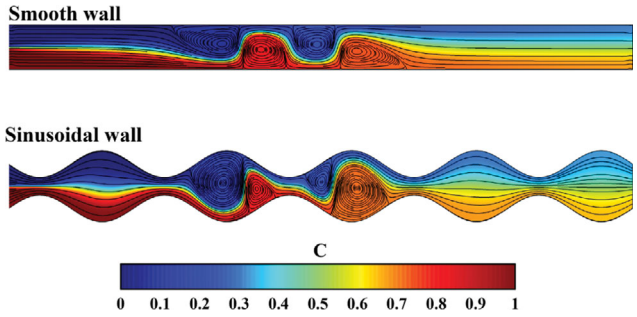

Fig. 13. Concentration distribution and streamlines in microchannels with straight and sinusoidal walls at φ=0.03%, d=1,000 μm, a=13.75 mm, and $\dot{Q}$=25 μl/min.

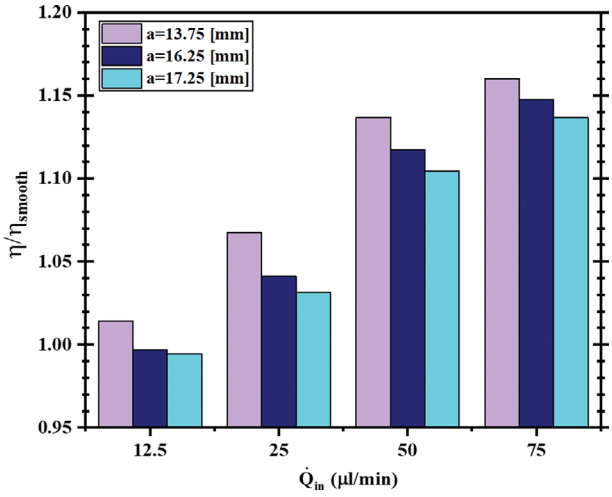

Fig. 14. The ratio of mixing index of the micromixer with sinusoidal walls to that of the micromixer with straight walls as a function of flow rate for different horizontal distances of the magnet from the inlet at φ=0.03%, and d=1,000 μm.

direction perpendicular to the flow direction. In general, it can be concluded that the hydrodynamic force overcomes the magnetic force, and the mixing index decreases. When the volumetric flow rate changes from the minimum to the maximum values, the mixing index decreases from 96% to 35%. The mixing index is always between 90 and 99% at low flow rate [16].

Even though the present study estimates the mixing efficiency in the presence of magnetic field for low Reynolds regime, two higher-order-of-magnitude Reynolds numbers are considered (Fig. 18(b)). It is demonstrated that as the Reynolds number is reduced,

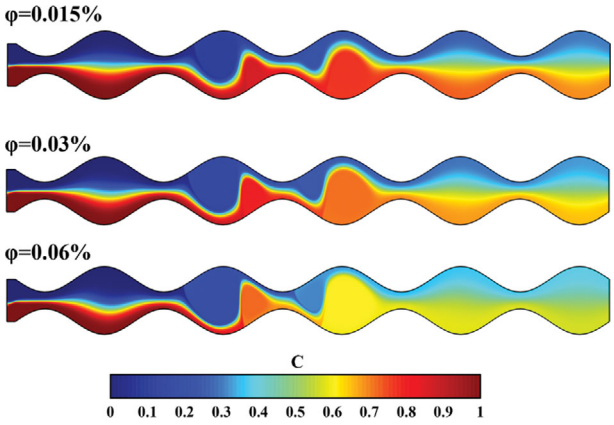

Fig. 15. Concentration distribution for different volume fractions of nanoparticles at d=1,000 μm, a=13.75 mm, and Q̇=25 μl/min.

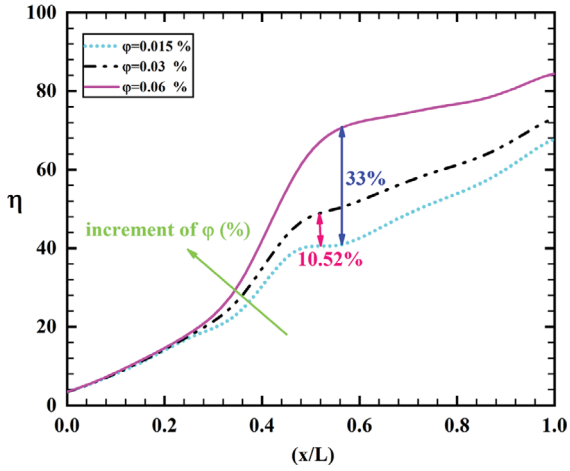

Fig. 16. Mixing index along the micromixer for different volume fractions of nanoparticles at d=1,000 μm, a=13.75 mm, and Q̇= 25 μl/min.

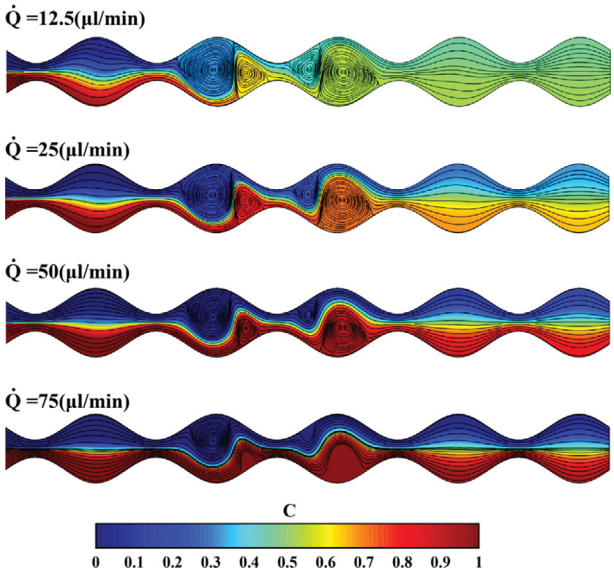

Fig. 17. Concentration distribution for different inlet flow rates at φ=0.03%, d=1,000 μm, and a=13.75 mm.

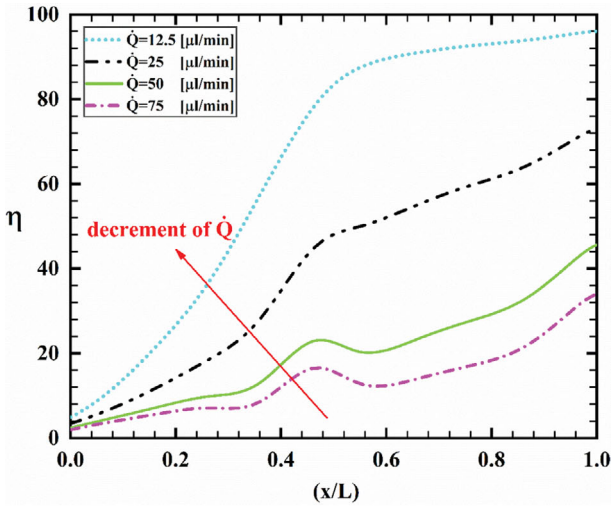

(a)

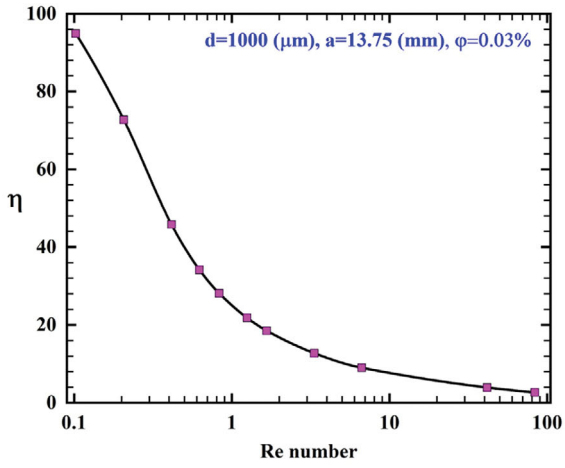

(b)

Fig. 18. (a) Mixing index along the micromixer for different flow rates at φ=0.03%, d=1,000 μm, and a=13.75 mm, (b) Mixing index for different Reynolds numbers.

mixing quality is improved, indicating that the present micromixer is more appropriate for low-Reynolds-number applications.

CONCLUSIONS

Different microfluidic devices use a magnetic field for mixing, separation, and pumping processes. In the present study, a two-dimensional combined active/passive micromixer was designed for experimental investigation. The micromixer has a microchannel with sinusoidal channel walls and a neodymium magnet is placed close to the microchannel. Water flow enters the microchannel from an inlet and ferrofluid flows with different flow rates from the other one. The results demonstrate that the presence of a magnetic field disrupts the regular motion of parallel streamlines and forms vortices. The mixing index is increased by 17.5% when a magnetic field is applied. Using the micromixer with sinusoidal walls leads to an increment in the mixing index by 16%. As the volume fraction of nanoparticles is enhanced, the mixing quality is improved. The horizontal and vertical distances of the magnet affect the gen-

eration of vortices and the mixing of water and ferrofluid. For example, when the magnet distance from the channel increases from 250 to 1,000 μm, the mixing index decreases by 2%, 33%, 67%, and 148% for flow rates of 12.5, 25, 50, and 75 μl/min, respectively. As the inlet flow rate increases, the magnetic force exerted on the ferrofluid cannot overcome the hydrodynamic force generated by the momentum, resulting in a reduction in the mixing index. Future work includes the experimental investigation of magnetic micromixers by employing permanent magnets and a Halbach array of magnets.

NOMENCLATURE

a	: horizontal distance of magnets [m]
B	: magnetic flux density distribution [W/m^2]
C	: concentration [mol/l]
d	: vertical distance of magnets [m]
d_{np}	: diameter of nanoparticle [m]
D	: diffusivity coefficient [m^2/s]
D_h	: hydraulic diameter [m]
$\vec{F}_{ext}$	: external force [N/m^3]
$\vec{F}_{mag,\,np}$	: magnetic force applied to the particle [N/m^3]
h	: microchannel height [m]
H	: magnetic field distribution [A/m]
L	: microchannel length [m]
m	: moment on the particle
M	: magnetization
P	: pressure [Pa]
r	: radius [m]
R_{np}	: the net rate of production of species
T	: temperature [K]
u	: velocity [m/s]
U_{in}	: inlet velocity [m/s]
V_p	: volume of the nanoparticle
x	: horizontal coordinate
y	: vertical coordinates
PDMS	: polydimethylsiloxane

Greek Symbols

η	: mixing efficiency [%]
φ	: volume fraction of nanoparticles
μ	: dynamic viscosity [Pa·s]
χ	: susceptibility
ρ	: density [kg/m^3]
μ_r	: relative permeability
μ_0	: vacuum permeability

Super- and Sub-scripts

f	: fluid
g	: gravity
ff	: ferrofluid
nf	: nanofluid
p	: particle
m	: magnetic force
mag	: magnitude
st	: surface tension

REFERENCES

1. M. Bayareh, M. N. Ashani and A. Usefian, *Chem. Eng. Process.*, **147**, 107771 (2020).
2. J. Nam, W. S. Jang and C. S. Lim, *Sens. Actuators B Chem.*, **258**, 991 (2018).
3. A. Usefian and M. Bayareh, *Meccanica*, **54**, 1149 (2019).
4. X. Huo and X. Chen, *J. Dispers. Sci. Technol.*, **42**, 1469 (2020).
5. A. Usefian, M. Bayareh and A. Ahmadi Nadooshan, *J. Heat Mass Trans. Res.*, **6**(1), 56 (2019).
6. E.-S. Shanko, Y. van de Burgt, P. D. Anderson and J. M. den Toonder, *Micromachines*, **10**, 731 (2019).
7. A. Munaz, M. J. Shiddiky and N.-T. Nguyen, *Biomicrofluidics*, **12**, 031501 (2018).
8. M. Hejazian, D.-T. Phan and N.-T. Nguyen, *RSC Adv.*, **6**, 62439 (2016).
9. M. Hejazian and N.-T. Nguyen, *Micromachines*, **8**, 37 (2017).
10. X. Wang, Z. Wang, V. B. Varma, Z. Wang, A. Ray and W. S. Lew, *IEEE Magn. Lett.*, **7**, 1 (2016).
11. C. Y. Wen, C. P. Yeh, C. H. Tsai and L. M. Fu, *Electrophoresis*, **30**, 4179 (2009).
12. Y. He, L. Luo and S. Huang, *Int. J. Mod. Phys. B*, **33**, 1950047 (2019).
13. A. Munir, J. Wang, Z. Zhu and H. S. Zhou, *IEEE Trans. Nanotechnol.*, **10**, 953 (2010).
14. M. Saadat, M. Ghassemi and M. B. Shafii, *Energy Sources A: Recovery Util. Environ. Eff.*, **42**, 1 (2020).
15. N. Azimi, M. Rahimi and N. Abdollahi, *Chem. Eng. Process.*, **97**, 12 (2015).
16. D. Nouri, A. Zabihi-Hesari and M. Passandideh-Fard, *Sens. Actuators A Phys.*, **255**, 79 (2017).
17. G.-P. Zhu and N.-T. Nguyen, *Lab Chip*, **12**, 4772 (2012).
18. C.-Y. Lee, W.-T. Wang, C.-C. Liu and L.-M. Fu, *Chem. Eng. J.*, **288**, 146 (2016).
19. M. Khosravi Parsa, F. Hormozi and D. Jafari, *Comput. Fluids*, **105**, 82 (2014).
20. S. Hossain, M. Ansari and K.-Y. Kim, *Chem. Eng. J.*, **150**, 492 (2009).
21. M. U. Javaid, T. A. Cheema and C. W. Park, *Micromachines*, **9**, 8 (2018).
22. A. Usefian and M. Bayareh, *Meccanica*, **55**, 1025 (2020).
23. A. Afzal and K.-Y. Kim, *Sens. Actuators B Chem.*, **211**, 198 (2015).
24. B. Mondal, S. K. Mehta, P. K. Patowari and S. Pati, *Chem. Eng. Process.*, **136**, 44 (2019).
25. A. Kausar, F. Sher, A. Hazafa, A. Javed, M. Sillanpää and M. Iqbal, *Int. J. Biol. Macromol.*, **161**, 1272 (2020)
26. T. Rashid, D. Iqbal, A. Hazafa, S. Hussain, F. Sher and F. Sher, *J. Environ. Chem. Eng.*, **8**, 104023 (2020).
27. T. Rasheed, S. Shafi, M. Bilal, T. Hussain, F. Sher and K. Rizwan, *J. Mol. Liq.*, **318**, 113960 (2020).
28. T. Rasheed, A. A. Hassan, F. Kausar, F. Sher, M. Bilal and H. M. N. Iqbal, *TrAC Trend. Anal. Chem.*, **132**, 116066 (2020).
29. J. Wu, Y. Cui, S. Xuan and X. Gong, *Microfluid. Nanofluid.*, **22**, 103 (2018).
30. D. Bahrami, S. Abbasian-Naghneh, A. Karimipour and A. Karimipour, *Math. Methods Appl. Sci.*, **43**, 1 (2020).
31. H. Brinkman, *J. Chem. Phys.*, **20**, 571 (1952).
32. C. Y. Wen, K. P. Liang, H. Chen and L. M. Fu, *Electrophoresis*, **32**,

3268 (2011).
33. Q. Cao, X. Han and L. Li, *Int. J. Appl. Electromagn. Mech.*, **47**, 583 (2015).
34. M. Nazari, S. Rashidi and J. A. Esfahani, *Int. Commun. Heat Mass Transf.*, **108**, 104293 (2019).
35. D. S. Bhandari, D. Tripathi and V. K. Narla, *Eur. Phys. J. Plus*, **135**(11), 1 (2020).
36. K. Ramesh, D. Tripathi, M. M. Bhatti and C. M. Khalique, *J. Mol. Liq.*, **314**, 113568 (2020).
37. N. S. Akbar, A. B. Huda, M. B. Habib and D. Tripathi, *Microsyst. Technol.*, **25**, 283 (2019).
38. M. Bayareh, *Proc. Inst. Mech. Eng.*, Part C (2020).
39. A. Shiriny and M. Bayareh, *Chem. Eng. Sci.*, **229**, 116102 (2020).